Electrochemical and Theoretical Investigation of Corannulene Reduction Processes

Carlo Bruno,[†] Rois Benassi,[‡] Alessio Passalacqua,[‡] Francesco Paolucci,[†] Claudio Fontanesi,*[,‡] Massimo Marcaccio,*[,†] Edward A. Jackson,[§] and Lawrence T. Scott*[,§]

INSTM, Section of Bologna, and Dipartimento di Chimica "G. Ciamician", Università di Bologna, via Selmi 2, 40126 Bologna, Italy; Dipartimento di Chimica, Università di Modena e Reggio Emilia, via Campi 183, 41100 Modena, Italy; and Chemistry Department, Merkert Chemistry Center, Boston College, Chestnut Hill, Massachusetts 02467-3860

Received: May 21, 2008; Revised Manuscript Received: November 14, 2008

The voltammetric generation of corannulene anions was investigated over a large range of experimental conditions comprising either "traditional" electrochemical solvents, such as dimethylformamide, acetonitrile, and tetrahydrofuran, or "unconventional" solvents, such as liquid ammonia, liquid methylamine, or liquid dimethylamine, and several different supporting electrolytes. Strong ion pairing effects were found to dominate the electrochemical generation of corannulene higher anions, and through the suitable choice of the solvent/electrolyte system, we observed, for the first time, the reversible electrochemical generation of up to the triply reduced corannulene. The standard potentials obtained experimentally compared rather well with the theoretical values calculated by ab initio and density functional methods, in which solvation and ion pairing effect were explicitly taken into account. In particular, the calculations considered the effect of the electrolyte cation size on ion pairing in order to rationalize the occurrence of the third reduction within the experimental potential window.

Introduction

The study of the reactivity of corannulene ($C_{20}H_{10}$, dibenzo[*ghi,mno*]fluoranthene) is a challenging topic due to the high symmetry of its geometrical structure, which heralds a peculiar electronic structure.[1] In fact, conformational analysis, microwave spectroscopy,[2] and X-ray diffraction studies[3] show that the most stable equilibrium geometry of the neutral closed-shell species is characterized by a slightly pyramidalized bowl-like structure featuring C_{5v} symmetry (Chart 1). Actually, the corannulene molecule may be considered as the upper one-third of a C_{60} molecule, with the residual valences of the more external carbon atoms saturated by hydrogen atoms.[4] Like other structurally similar systems (ammonia is the classic example), corannulene is characterized by inversion dynamics, which have been investigated in solution by NMR spectroscopy.[5] Moreover, corannulene is particularly appealing as a synthetic intermediate from which to build extremely interesting molecular structures,[6] with nontraditional geometric as well as electronic properties of potential use in the design of new materials.[7] For instance, neutral radicals with bowl-shaped structures, as also obtained in the case of fullerene derivatives, have been obtained as unstable molecules in solution.[8] Quite recently, a bowl-shaped neutral radical incorporating a corannulene system has been designed and synthesized for the first time as a stable solid in air. In this case, it has been established that an appreciable amount of spin delocalization extends onto the corannulene unit's curved surface.[9] Corannulene chemistry has also started to become a very intriguing research subject in the field of metal complexes with π-electron curved surface ligands.[10]

CHART 1: Corannulene Molecule and Its Bowl-Shaped C_{5v} Symmetry (n = 0, 1−, 2−, 3−, 4−)

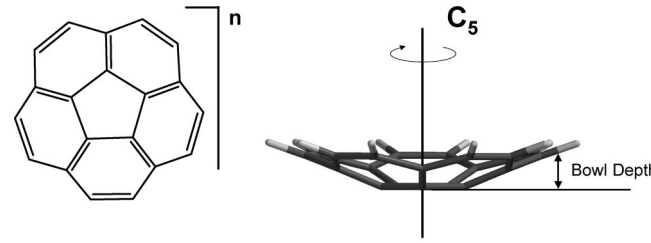

The lowest unoccupied molecular orbital (LUMO) of corannulene is low-lying and doubly degenerate; this fact accounts for the stability of the reduced species. In fact, this expected behavior is experimentally fulfilled: (i) the electron affinity is positive (0.50 eV);[11] (ii) negatively charged corannulene species have been studied both under vacuum, by means of electron transmission spectroscopy (ETS),[12] and in homogeneous condensed phase, electrochemically,[13] as well as by the electron spin resonance (ESR) technique.[14] In principle, some aspects of the electrochemical behavior should be shared in common with C_{60}. The latter has 3-fold degenerate LUMOs, in agreement with the experimental observation that C_{60} can accommodate up to six extra electrons in solution.[15] In fact, the electrochemical generation of only the anion and dianion of corannulene has been reported so far,[13] while its tetraanion has been prepared with alkali metal in THF and observed by NMR spectroscopy.[14,16,17]

Against this backdrop, the present study aimed at identifying suitable conditions for the electrochemical reversible generation of the elusive higher anions of corannulene and for their thorough characterization. In the search for the best conditions for the stabilization of such highly charged species, a large variety of either traditional electrochemical aprotic solvents, such

* Corresponding authors. E-mail: claudio.fontanesi@unimore.it (C.F.), massimo.marcaccio@unibo.it (M.M.), lawrence.scott@bc.edu (L.T.S.).
[†] Università di Bologna.
[‡] Università di Modena e Reggio Emilia.
[§] Boston College.

10.1021/jp8045092 CCC: $40.75
Published on Web 01/27/2009

as dimethylformamide, acetonitrile, and tetrahydrofuran, or "unconventional" solvents, such as liquid ammonia, liquid methylamine, or liquid dimethylamine, were used. Furthermore, several supporting electrolytes were employed with the aim of investigating the effect of countercation size on the stability of the electrogenerated anions. Our study revealed in fact that the voltammetric generation of corannulene anions is strongly influenced by ion pairing effects, and through the suitable choice of the solvent/electrolyte system, we observed, for the first time, the reversible electrochemical generation of the triply reduced corannulene.

In order to have a better insight into the electrochemical behavior of corannulene, the electrochemical investigation was paralleled by quantum chemical calculations, performed at ab initio and DFT levels of theory, that provided electron affinity and standard reduction values to compare with the experimental values. In particular, high-quality thermodynamic quantities were calculated within the CBS4MB paradigm.[18] The calculations took into account solvent and ion pairing effects explicitly and provided a tight agreement between the experimental and theoretical results. Importantly, calculations also predicted that, in the condensed phase, the electrochemical generation of corannulene tetraanion cannot be accomplished because of the very large negative standard potential that locates the generating process outside the currently available experimental potential windows.

Experimental Section

Chemicals and Electrochemical Measurements. Corannulene was synthesized according to the three-step procedure by Scott et al.[19]

Tetrabutylammonium hexafluorophosphate (TBAH), tetraethylammonium tetrafluoroborate (TEAB), tetramethylammonium tetrafluoroborate (TMAB), tetrabutylammonium bromide (TBABr), potassium bromide (KBr), sodium tetrafluoroborate ($NaBF_4$), lithium hexafluorophosphate ($LiPF_6$), lithium hexafluoroarsenate ($LiAsF_6$), lithium trifluoromethanesulfonate (LiTFS), and lithium tetrakis(pentafluoroaryl)borate (LiFAB; containing two tetrahydrofuran solvent molecules) were used as received as supporting electrolytes, and all were electrochemical or analytical grade from Fluka. The electrolyte tetraethylammonium tetrakis(pentafluoroaryl)borate (TEAFAB) was synthesized by the metathesis reaction between tetraethylammonium bromide in ethanol and LiFAB in water and purified twice by dissolution in ethanol and recrystallization with water. Dry vacuum-distilled *N,N*-dimethylformamide (DMF) was purified using sodium anthracenide in order to remove any traces of water and oxygen, according to the method of Aoyagui.[20] Acetonitrile (ACN) and tetrahydrofuran (THF) were purified and dried as previously reported,[21] stored in a specially designed Schlenk flask and protected from light.

Ammonia (NH_3), dimethylamine (DMA), and methylamine (MA) were purified and dried by refluxing over activated alumina super I basic (ICN Biomedicals) at the corresponding boiling temperature and then passed through an activated alumina column under reduced pressure, just before condensing the vapor into the electrochemical cell.

All the other (conventional) solvents were distilled via a closed system into an electrochemical cell containing the supporting electrolyte and the species under examination, immediately before performing the experiment. All other chemicals were of reagent grade. Electrochemical experiments were carried out in an airtight single-compartment cell described elsewhere,[15b] using platinum as working and counter electrodes and a silver spiral as a quasi-reference electrode. The drift of the quasi-reference electrode was negligible during the time required for an experiment. All the half-wave potentials ($E_{1/2}$) have been directly obtained from cyclic voltammetric curves as averages of the cathodic and anodic peak potentials and by digital simulation for those processes, which are not Nernstian, or for processes closely spaced in multielectron voltammetric peaks. The $E_{1/2}$ values, referenced to the aqueous saturated calomel electrode (SCE, which is 0.241 V vs NHE, i.e., the normal hydrogen electrode[22]), have been determined by adding ferrocene at the end of each experiment as an internal standard and measuring them with respect to the ferrocinium/ferrocene couple standard potential. The temperature-dependent ferrocinium/ferrocene couple standard potential was measured with respect to SCE by a nonisothermal arrangement according to the method outlined by Weaver et al.[23] The potentials thus obtained were not corrected for the two unknown contributions: (i) the liquid junction potential between the organic phase and the aqueous SCE solution and (ii) the potential due to the thermal gradient existing between the SCE, at room temperature, and the low temperature test solution.

The cell containing the supporting electrolyte and the electroactive compound was dried under vacuum at 373−393 K for at least 60 h before each experiment. The pressure measured in the electrochemical cell prior to performing the trap-to-trap distillation of the solvent was typically $(1-2) \times 10^{-5}$ mbar. Voltammograms were recorded with an AMEL model 552 potentiostat or a custom-made fast potentiostat[24] controlled by an AMEL model 568 programmable function generator. The potentiostat was interfaced to a Nicolet model 3091 digital oscilloscope, and the data were transferred to a personal computer by the program Antigona.[25] Minimization of the uncompensated resistance effect in the voltammetric measurements was achieved by the positive-feedback circuit of the potentiostat. Digital simulations of the cyclic voltammetric curves were carried out either by Antigona or DigiSim 3.0. The determination of the potentials, for the irreversible processes, was obtained by digital simulation of the cyclic voltammetric curves[26] utilizing a best-fitting procedure of the experimental curves recorded at different scan rates spanning over, at least, 2 orders of magnitude.

Computational Details. Ab initio molecular orbital calculations were performed using the Gaussian 03 suite of program.[27] Screening calculations on corannulene and its four anions were performed by using a wide range of basis sets (Midi, 6-31G**, 6-31+G*, cc-pVTZ, and Aug-cc-pVTZ) in combination with MP2, MP3, B3PW91, and B3LYP post-SCF and DFT methods. Detailed theoretical results, obtained at two different levels of accuracy, are presented and discussed. In one case, the geometries of the neutral corannulene, the anions, and the clusters made of corannulene (neutral, 1−, 2−, 3−, 4− anions) and the electrolyte cation (i.e., Li^+, TMA^+, and TBA^+) were optimized at the B3PW91/Midi level of theory. The relevant analytic harmonic vibration frequency and electron affinity calculations were also performed. A more accurate approach was pursued for the corannulene (neutral and its anions) and the corannulene/Li^+ cluster by performing the geometry optimization, together with the relevant analytic harmonic vibration frequency calculations, at the B3LYP/6-31G** level of theory; electron affinity values (at $T = 0$ K) were calculated at both the B3LYP/cc-pVTZ and B3LYP/Aug-cc-pVTZ//B3LYP/6-31G** levels of theory.

The small size Midi basis set has been selected as a good compromise of speed and accuracy. It was optimized paying

SCHEME 1: Thermodynamic Cycle for the Calculation of the Redox Potentials vs NHE

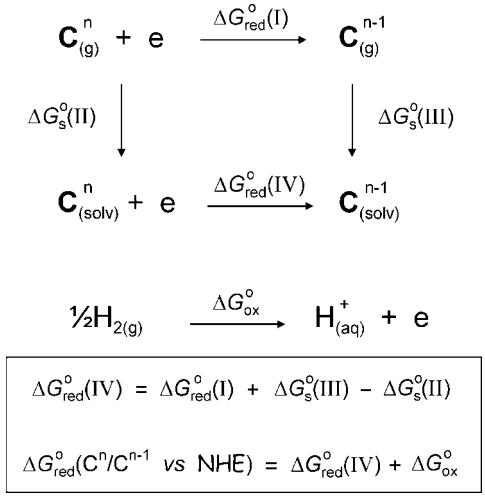

particular attention to charged and sizable molecular systems.[18] Indeed, UB3PW91/MIDI-based calculations produced satisfactory results of standard potential values, as shown by Cramer and Truhlar.[28] Recently, B3LYP/cc-pVTZ//B3LYP/6-31G**-based calculations on a series of molecular systems, smaller than corannulene, have shown to reproduce accurately electrochemical potentials.[29] Analytic harmonic vibration frequency calculations were performed to characterize the nature of stationary points on the potential energy surface, with the aim to determine the suitable thermodynamic quantities prone to conformational analysis and redox potential calculations. Geometry optimizations in the gas phase were used to perform solvation free energy calculations (solvation free energies have been obtained at the B3PW91/Midi and B3LYP/cc-pVTZ levels of theory) of the various species involved in the determination of redox potentials, following the Barone's polarizable conductor model (CPCM) method,[30] which is based on the polarized continuum model (PCM) of Tomasi and co-workers.[31]

Theoretical reduction potentials reported in this paper have been calculated at 298 K at the B3PW91/Midi level of theory approach, while both variations in the solvent properties[32] (dielectric constant and density) and the "full" thermal contribution[33] as a function of the temperature have been accounted for within the B3LYP/cc-pVTZ//B3LYP/6-31G** approach (i.e., allowing for an "exact" calculation of the reduction potential within the intrinsic limitations of this selected level of the theory and save the validity of the extra-thermodynamic value of ΔG°_{ox} relevant to the redox couple H^{+}/H_2; see Scheme 1).

Results and Discussion

In this work the sequence of four one-electron reductions involving corannulene (**C**) was studied both experimentally and theoretically; each electrochemical elementary step is assumed to occur through an outer-sphere reversible electron transfer process, involving a single-electron uptake reaction. The sequence can thus be summarized as a series of four reactions, in which each successive reductive step is associated with a relevant standard reduction potential value.[22]

Electrochemistry. With the aim to investigate the properties and electrochemical behavior of higher **C** anions, aprotic solvents and very dry conditions were chosen to ensure wide negative potential windows and very high stabilization of the electrogenerated anions. The potentials of the first and second reductions in ACN have been previously reported.[13] We reinvestigated the voltammetric behavior of **C** in such a medium confirming that, in spite of the carefully purified solvent and the ultradry conditions used, which allow a very large negative potential window (down to −3.1 V vs SCE),[21a] (i) no further reduction processes could be detected and (ii) the second reduction was affected by a follow-up reaction causing partial irreversibility of the voltammetric peak (see Figure S1 in Supporting Information), even at low temperature and sweep rate as high as 50 V/s. The potentials $E_{1/2}$ of the two processes are in Table 1. Whereas the first reduction compares very well with the values determined by Janata[13a,34] and Seiders[13b,34] (10−30 mV of discrepancy), the second process at −2.61 V (determined by digital simulation with an ECE mechanism[26]) is 130−200 mV more negative.[34] This potential shift toward less negative values is consistent with a rather fast chemical reaction coupled to the electron transfer. The investigation was then carried out in a variety of solvents that allow large negative potentials and are known for their ability to stabilize electrogenerated anions. Thus, "conventional" solvents for electrochemistry, such as DMF and THF, as well as less commonly used ones, such as liquid ammonia (liq-NH_3) and liquid alkylamines, i.e., DMA (liq-DMA) and MA (liq-MA), were employed. Furthermore, the choice of the supporting electrolyte was found to be critical to stabilize the electrogenerated anions. This finding is in line with the observation that corannulene can be chemically reduced by metallic lithium in THF to its tri- and tetraanions.[14,16] The electrogeneration of higher anions of corannulene was facilitated by the choice of supporting electrolytes with small countercations.

TABLE 1: Experimental Half-Wave Reduction Potentials, $E_{1/2}$/V vs SCE (Which is 0.241 V vs NHE),[22,37] of Corannulene in Different Electrolyte/Solvent Systems[a]

electrolyte/solvent	T/K	$E_{1/2}$(I)/V	$E_{1/2}$(II)/V	$E_{1/2}$(III)/V
TBAH/ACN	298	−1.90	−2.61[d,f]	
TBAH/THF	298	−1.89	−2.47	
TBAH/DMF	298	−1.87	−2.57	
TEAB/DMF	213	−1.87	−2.41	−3.13[c,f]
TMAB/DMF	213	−1.88	−2.42	−3.01
$LiAsF_6$/DMF	213	−1.83	−2.45	−2.62[d,e]
TBABr/liq-DMA	193	−1.83	−2.28	−3.12
TBABr/liq-MA	193	−1.80	−2.37	−3.16[c,f]
LiTFS/liq-NH_3[b]	213	−1.86	−2.39	−2.53[d,e]

[a] Working electrode: platinum; 1 mM corannulene in 0.07 M electrolyte solution. [b] 0.25 mM (saturated solution) corannulene solution. [c] Irreversible reduction process occurring at the edge of the useful potential window. [d] Irreversible process. [e] Cathodic peak potential value. [f] $E_{1/2}$ value obtained by digital simulation.[26]

In Figure 1a the cyclic voltammetric (CV) curve of corannulene in TBAH/DMF, recorded at low temperature, shows two one-electron reduction peaks within the useful potential window, extending down to about −3.1 V vs SCE. The first voltammetric wave is a Nernstian process, whereas the second one reveals some degree of electrochemical irreversibility. The voltammetric behavior is maintained also at room temperature, and it is still possible to observe two one-electron processes, although the second reduction is partially affected by a follow-up chemical process. This can be safely ascribed to the high basicity of the corannulene dianion, which abstracts a proton from the solvent/electrolyte system. By increasing the scan rate, the second process becomes chemically reversible.

A very similar behavior was observed in THF (Figure S2 in Supporting Information): two one-electron reductions were observed, the second of which was characterized by slow

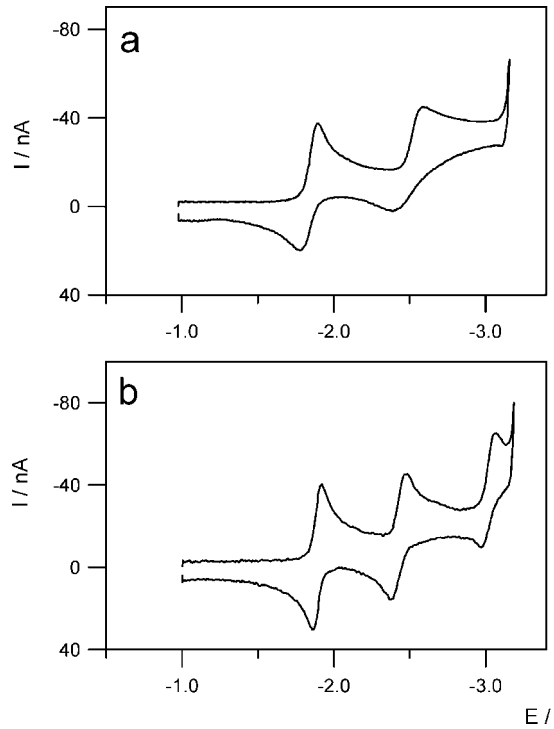

Figure 1. Cyclic voltammetric curves of corannulene 1 mM in (a) 0.07 M TBAH/DMF solution (T = 218 K) and (b) 0.08 M TMAB/DMF solution (T = 213 K). Working electrode Pt disk 125 μm (diameter); reference electrode SCE; scan rate = 1 V/s.

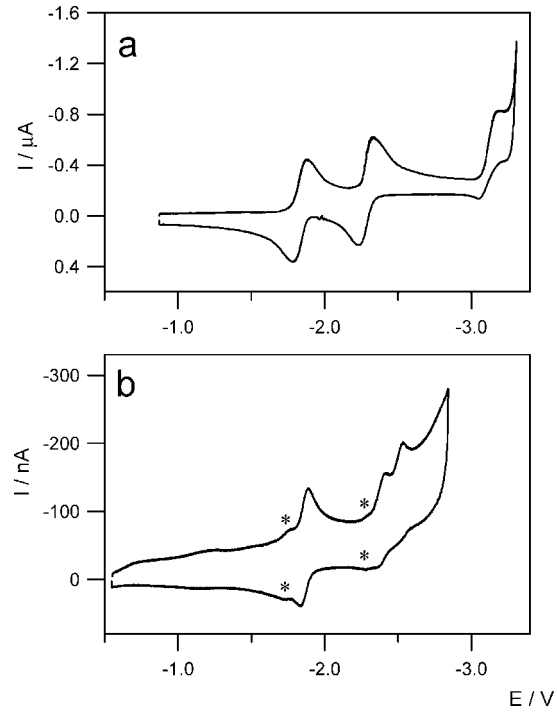

Figure 2. Cyclic voltammetric curves of corannulene (a) 1 mM in 0.08 M TBABr/liq-DMA solution (T = 193 K); (b) 0.25 mM (saturated solution) in 0.07 M LiTFS/liq-NH_3 solution (T = 213 K). Working electrode Pt disk 0.5 mm (diameter); reference electrode SCE; scan rate = 0.2 V/s. The small peaks (shoulders) close to the first two main reductions (labeled by asterisks) are due to the presence of a small amount of the chlorinated precursor of corannulene as impurity.[41]

electron transfer kinetics. The corresponding $E_{1/2}$ values are reported in Table 1.

A further step to achieving the electrochemical generation of more highly reduced corannulene species involved changing the electrolyte. It is known that the electrolyte cation can affect the heterogeneous electron transfer through both the structure of the double layer[35] and the possible formation of ion pairs.[36] Since the tri- and tetraanion have been generated in THF by the chemical reduction of corannulene with metallic lithium,[14,16] as mentioned above, electrochemical experiments were pursued in the same solvent using Li^+ as the electrolyte. Unfortunately, the discharge of lithium ions caused a narrowing of the available potential window,[36d] thus preventing the detection of any tri- and tetraanion of corannulene.

The possibility of dissolving different electrolytes in DMF allowed us to investigate the effect of the electrolyte cation on the reductions of corannulene. When the size of the tetraalkylammonium was reduced (i.e., changing from TBA^+ to TEA^+) and the solution was kept at low temperature, a third one-electron process appeared as a shoulder at the edge of solvent/electrolyte discharge (see Figure S3 in Supporting Information). An $E_{1/2}$ at 3.13 V was determined by digital simulation of the voltammetric curve. Finally, as the cation size is further decreased (electrolyte TMA^+), the third reduction can be easily detected at −3.01 V (Figure 1b).

This third process, observed in TMAB electrolyte, is chemically reversible, although it appears to be a sluggish electron transfer, similar to the second reduction. Comparison of the $E_{1/2}$ values reported in Table 1, for DMF solutions with different electrolytes, shows that, while the first process is not affected by the type of electrolyte cation, the second reduction becomes about 150 mV easier when the electrolyte is changed from TBAH to TEAB or TMAB, and a comparable effect can be noted for the third reduction, for which a 120 mV shift of the standard potential toward less negative values was obtained on passing from TEAB to TMAB.

Voltammetric measurements in $LiAsF_6$/DMF (Figure S4 in the Supporting Information) highlight an even more dramatic effect on the third process that, in this case, moves very close to the second reduction, while the third reduction is chemically irreversible.

Liq-DMA has been used as a solvent for electrochemistry to investigate the reductions of a series of aromatic hydrocarbons,[38] since it is known to stabilize anions and it allows the generation of reduced species at very negative potentials. Thus, corannulene was studied in TBABr/DMA at low temperature (193 K), and the CV curve (Figure 2a) shows three one-electron reductions. The first process is reversible while the second and third reductions are characterized by slower electron transfers. Moreover, the last one is also partially affected by a chemical reaction. It is worth noting that the solvation effect stabilizes the trianion, moving its reduction potential toward less negative values within the useful potential window.

The effects of the solvent and the electrolyte cation on the stability of the corannulene anions have been further probed using liquid ammonia as solvent and Li^+ as electrolyte. The CV curve in Figure 2b shows a voltammetric pattern which is very reminiscent of that recorded in Li^+/DMF. In Li^+/liq-NH_3 the second reduction occurs at a potential slightly less negative with respect to that of the corresponding process in DMF with TEA^+, TMA^+, and Li^+ electrolytes, while the third electron uptake is 90 mV easier than in Li^+/DMF. This could be attributed to a stronger ion pairing effect in liq-NH_3 with respect to DMF.

Concerning the kinetics of the heterogeneous electron transfers of corannulene, a very similar behavior was observed in all electrolyte solutions investigated in this work, with the second

TABLE 2: Calculated Bowl Depth (see Chart 1) Values and Mulliken Charges on the H Atoms for Corannulene and Its Four Anions in Gas Phase and Two Different Solvents, Together with the Activation Gibbs Free Energy Values for Bowl-to-Bowl Inversion (UB3PW91/Midi) at 298 K

	$\Delta G^{\neq}$/kcal mol^{-1}				
	gas phase	DMF	THF	bowl depth/Å	Mulliken H charge
C	6.5	9.9	12.5	0.78	0.19
$\mathbf{C}^{1-}$	4.6	3.2	3.6	0.70	0.14
$\mathbf{C}^{2-}$	2.8	2.9	2.6	0.57	0.08
$\mathbf{C}^{3-}$	1.8	2.1	2.5	0.41	0.01
$\mathbf{C}^{4-}$	1.5	1.5	1.6	0.16	−0.05

and the third (when observed) electron transfer being intrinsically slow in comparison to the first one. This is suggested by the analysis of the shape and other features of the corresponding voltammetric peaks,[39] and it can be attributed to a larger reorganization energy of the second reduction compared to that of the first one.[39] Most likely, such an energy is related, at least in part, to a more pronounced conformational change by the introduction of the second electron.[40] As is described in the following section, quantum-chemical calculations show that going from the species $\mathbf{C}^{1-}$ to $\mathbf{C}^{2-}$ the bowl geometry is flattened (bowl depth decreases) nearly twice as much as that caused by the introduction of the first electron on the neutral molecule (see Table 2).

Theoretical Calculation of the Redox Potentials. The doubly degenerate nature of the LUMO of the neutral closed-shell species will induce distortion in negatively charged corannulene (Jahn−Teller effect). The distortion breaks the high C_{5v} symmetry and reduces the geometric orbital symmetry to C_s, splitting the degenerate LUMOs into a pair of orbitals with different symmetry A′ and A. To probe this effect, we optimized the geometry of the neutral corannulene and the anions without symmetry constraints, eventually obtaining minima of C_{5v} and C_s symmetry, respectively. Concerning the neutral, closed-shell corannulene state, there is wide agreement in the literature on the fact that the most stable molecular conformation is a bowl-like structure characterized by C_{5v} symmetry.[42] We obtained a result in line with the aforementioned literature findings following a full geometry optimization procedure, without any initial symmetry constraint, at the UB3PW91/Midi level of theory. Then, a further refinement of the geometry search allowed us to find of an equilibrium molecular geometry corresponding to an exact C_{5v} symmetry, where the internal five-carbon ring is not on the same plane of the carbons belonging to the external ring (Chart 1). To account for the lowering of the molecular frame symmetry from C_{5v} to C_s upon injection of an electron, we optimized the corannulene anion geometry without symmetry constraints, starting from the C_{5v} geometry relevant to the neutral closed-shell species. Yet, following this initial geometry optimization procedure, further refinement of the geometry corresponding to the minimum in energy allowed us to individuate a final equilibrium conformation of C_s symmetry. Thus, the lowering of the molecular symmetry splits the two degenerate LUMOs into an A′ SOMO (singly occupied molecular orbital) and an A″ LUMO. The same procedure was also followed for the geometry optimization of the 2−, 3−, and 4− ions; in all cases the most stable optimized geometries are characterized by C_s symmetry, always featuring a bowl-like shape.

An aspect of the corannulene dynamic behavior which must be studied for a detailed understanding of its redox characteristics is its bowl-to-bowl inversion process, since it is of primary importance to ascertain the relative stability of the conformations generated by such a process and to evaluate their possible effect on electrochemical kinetics and electrochemically induced reactions. Table 2 sets out theoretical results concerning the bowl-to-bowl inversion process, both in vacuum and in the DMF and THF solvents (CPCM model),[30] for differently charged species, from the neutral corannulene up to the tetraanion.

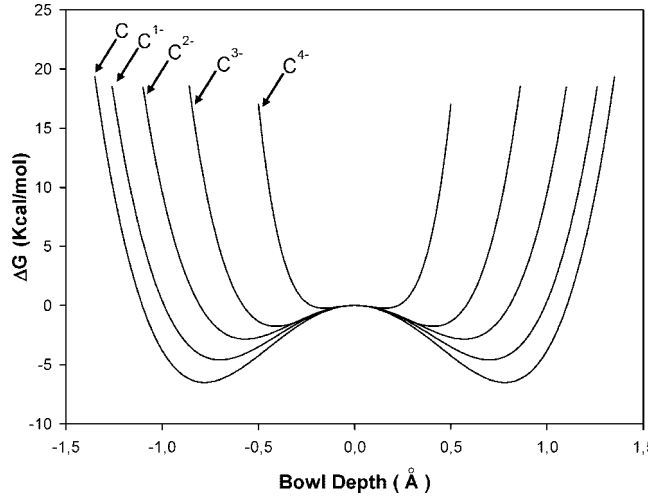

Figure 3. Energy diagram for the bowl-to-bowl inversion barrier for corannulene (**C**) and its four anions $\mathbf{C}^n$ ($n = 1-, 2-, 3-, 4-$) calculated in a vacuum.

In the case of the neutral closed-shell species, a fairly good agreement is found between the experimental value and our theoretical result for the activation energy for the bowl-to-bowl inversion process: 11.5 ± 0.5 kcal mol^{-1} is the value determined experimentally in DCM, evaluated by NMR spectroscopy,[5b] whereas our theoretical value (B3PW91/Midi including CPCM solvent) is 11.2 kcal mol^{-1}. Referring to the dynamic behavior of corannulene in the vacuum phase, a reasonable agreement is obtained also between theoretical results from the literature, falling in the 8−16 kcal mol^{-1} range, and our (B3PW91/Midi in the vacuum) value of 6.5 kcal mol^{-1} for the bowl-to-bowl activation energy barrier (see Figure 3).

A comparison of geometric and electronic energy results indicates that an increase of the net negative charge of the system (0, 1−, 2−, 3−, 4−) reduces both the bowl depth and the barrier height for ring inversion.[43] This has a twofold origin: an *electrostatic* and an *orbital* contribution. The analysis of the net charges shows that the majority of the excess negative charge, introduced by each successive one-electron addition, is localized on the most external carbon and hydrogen atoms (rim side), reducing, in this way, the above-mentioned repulsive Coulombic interaction.[42] In fact, the dimension of corannulene depends on the charge, such that the larger the negative charge, the larger the molecular dimension.

Moreover, inspection of the SOMO shape (it is found that Midi, 6-31G**, 6-31+G*, cc-pVTZ, and Aug-cc-pVTZ basis sets all yield the same qualitative picture) shows a multicenter bonding character, which extends over hub, spoke, rim, and flank carbon−carbon bonds, and is of π-type nature (Figure 4). Thus, carbons involved in the bonding part feel compelled to lie on the same geometric plane. From this perspective, it appears that the corannulene electronic system should not be viewed as an abnormal species constituted by an aromatic ring of five atoms within an almost independent surrounding 15-carbon aromatic system. Such a picture is not consistent with the aforementioned tendency to assume a more flat geometry, as in the case of the anions.

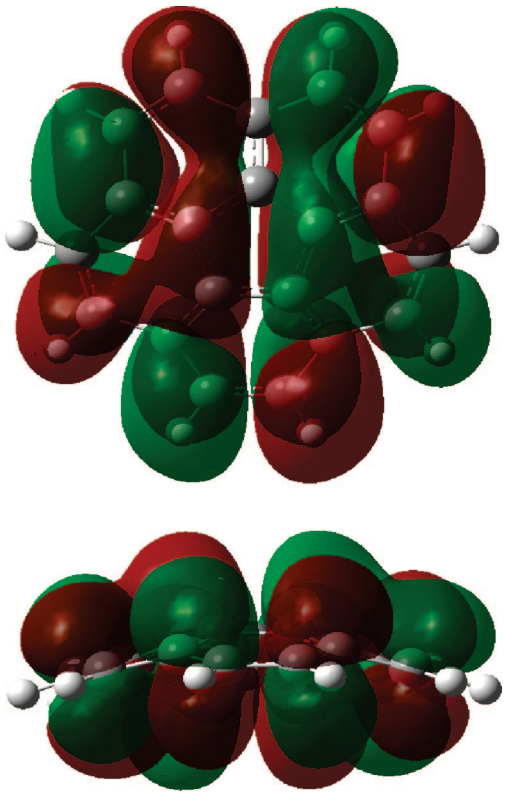

Figure 4. Singly occupied molecular orbital (SOMO) surfaces of $\mathbf{C}^{1-}$ calculated at the B3PW91/Midi level of theory.

For the sake of comparison between different levels of theory, the corannulene electron affinity has been calculated using a rather large combination of basis sets, by both DFT and post-SCF (MP2 and MP3) methods. The results are collected in Table S1 (Supporting Information). Experimentally, it is found that EA = 0.5 eV,[11] and a satisfactory agreement is obtained in the case of B3PW91/Midi, B3PW91/6-31G*, and B3LYP/6-31G* calculations.

The results from the literature, where the UB3PW91/Midi level of the theory is found well suited to study organic molecules bearing a net charge,[28] together with our screening results for the bowl-to-bowl inversion and electron affinity values, suggest the choice of the Midi basis set and B3PW91 DFT method as suitable choices for our further calculations.

Concerning the electrochemical behavior of corannulene, the calculation of the standard potential, $E°$, can be pursued by using the Nernst equation: $\Delta G° = -FE°$. The strategy of the method followed in this work is based on the use of a classical thermodynamic cycle (Scheme 1), as proposed by Cramer and Truhlar,[28] where $n = 0, 1-, 2-, 3-$. The gas-phase Gibbs energies of both reactants and products, as well as the relevant solvation free energy, are the quantities involved in the calculation of the redox potential. The standard reduction potential of the $\mathbf{C}^n/\mathbf{C}^{n-1}$ couple in solution is calculated as the sum of individual contributions[37] (Scheme 1). The free Gibbs energy variation of the whole reduction process is the sum of the two contributions relevant to the corannulene and hydrogen reduction half-reactions; thus, $\Delta G°_{red}(\mathbf{C}^n/\mathbf{C}^{n-1}$ vs NHE) = $\Delta G°_{red}(\mathrm{IV}) + \Delta G°_{ox}$. In Scheme 1, step IV represents the half-reaction Gibbs energy variation of the reduction process in solution: $\Delta G°_{red}(\mathrm{IV}) = \Delta G°_{red}(\mathrm{I}) + \Delta G°_{s}(\mathrm{III}) - \Delta G°_{s}(\mathrm{II})$, where $\Delta G°_{red}(\mathrm{I}) = \mathrm{EA} + \Delta G°_{evr,gas}$ ($\mathbf{C}^n_{gas} + e \rightarrow \mathbf{C}^{n-1}_{gas}$; see Table S2 in the Supporting Information). The $\Delta G°_{evr,gas}$ ($\mathbf{C}^n_{gas} + e \rightarrow \mathbf{C}^{n-1}_{gas}$) term reflects the difference in thermal contributions to the Gibbs energy of **C** due to changes in the electronic, vibrational, and rotational partition functions upon reduction. In B3PW91/Midi calculations the thermal quantity $\Delta G°_{evr,gas}$ was neglected since its contribution has been shown, at a first aproximation, to be quantitatively of little importance in previous cases.[28] $\Delta G°_{s}(\mathrm{III})$ and $\Delta G°_{s}(\mathrm{II})$ are the solvation Gibbs energies of the reduced and oxidized species, respectively, which are the two lateral branches of Scheme 1 (Table S3 in the Supporting Information).

TABLE 3: Theoretical Reduction Standard Potentials (vs SCE, Which is 0.241 V vs NHE; T = 298 K, except Where Explicitly Indicated[a]) Calculated at UB3PW91/Midi Level of Theory (Including the BSSE Correction for the TBA^+/DMF, TMA^+/DMF, and Li^+/DMF Cases) Using Scheme 1

solvent	$E°$(I)/V	$E°$(II)/V	$E°$(III)/V	$E°$(IV)/V
ACN	−2.39	−3.33	−4.31	−5.22
THF	−2.62	−3.85	−5.16	−6.45
DMF	−2.27	−2.99	−5.80	−6.96
TBA^+/DMF	−2.35	−2.95	−3.99	−4.52
TMA^+/DMF	−2.36	−2.86	−3.68	−4.68
Li^+/DMF	−1.69	−2.60	−3.21	−4.76[b]
liq-DMA (T = 193 K)	−2.12	−3.12	−4.04	−4.88
liq-NH_3 (T = 213 K)	−2.28	−2.99	−3.90	−4.68

[a] Only the solvation free energy is evaluated at the indicated temperature. [b] The calculations for the cluster [$\mathbf{C}^{4-}/Li^+$] did not converge within the same methodology used for the other clusters; thus, the theoretical standard potential for the fourth reduction $E°$(IV) has been calculated for a geometry which is not a true minimum, and hence it has to be considered a crude estimation.

Different solvent systems have been considered: ACN, THF, DMF, TBA^+/DMF, TMA^+/DMF, Li^+/DMF, liq-DMA, liq-MA, and liq-NH_3. A value of 4.44 eV has been assigned to the $\Delta G°_{ox}$ of the couple H^+/H_2.[44a,45] In fact, the calculation of the $\Delta G°_{red}$(IV) term is dominated by the electron affinity value. Table 3 sets out $E°$ values calculated at the UB3PW91/Midi level of theory. Focusing on the values of the first three lines together with those of the last two of the same Table 3, it is evident that the theoretical potentials are not in tight agreement with those experimentally obtained. On average, the theoretical potentials are 0.45 V more negative than the experimental values. Nevertheless, a better quantitative agreement is found when comparing experimental and theoretical $E°$(II) − $E°$(I) differences, indicating that the shift and the relative ordering of the potentials are calculated better than the absolute values.

The reliability of UB3PW91/Midi results has been confirmed by calculating EA relevant values at higher levels of theory (Table S4, Supporting Information). A close agreement occurs for UB3PW91/Midi, UB3PW91/6-31G*, and UB3LYP/6-31G* results. Unexpectedly, the use of diffuse orbitals and MP2/MP3 post-SCF methods yield results that are not physically acceptable. For instance, UB3PW91/6-31+G* and UB3LYP/6-31+G* potentials referring to formation of the trianion and tetraanion of corannulene are more positive than the first and second reduction potentials (highlighted values in Table S4, Supporting Information), a result which is inconsistent with the experimental evidence; the UMP2/6-31G* and UMP3/6-31G* calculations yield worse absolute potentials with respect to UB3PW91/Midi, UB3PW91/6-31G*, and UB3LYP/6-31G* calculations. Moreover, at variance with the DFT-based calculations, UMP2/6-31G*, UMP3/6-31G*, UMP2/6-31+G*, and UMP3/6-31+G* calculations heavily suffer in achieving self-consistency. However, a remarkable improvement in the matching between the calculated and experimental values can be obtained by using a higher DFT level of theory, as B3LYP/cc-pVTZ//B3LYP/6-31G** (vide infra).

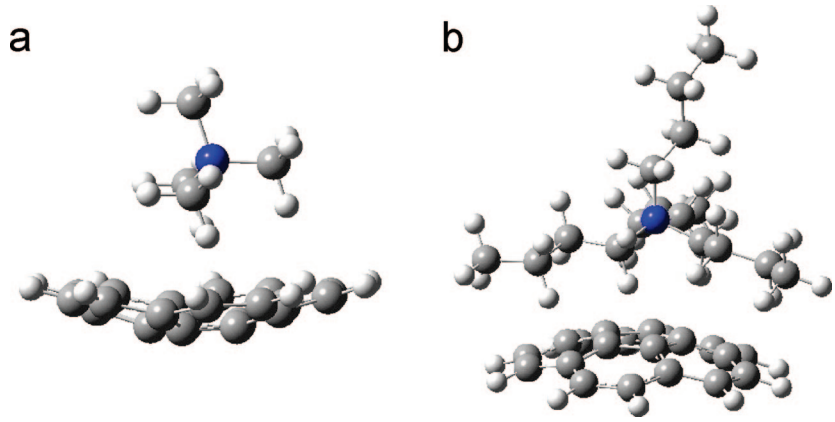

Figure 5. Structures of the neutral clusters optimized at the UB3PW91/Midi level of the theory for (a) [$\mathbf{C}^{-}$/TMA^{+}] and (b) [$\mathbf{C}^{-}$/TBA^{+}].

Ion Pair Modeling. One of the most important aspects of this theoretical approach is the possibility to provide a reliable estimation of quantities that are not experimentally accessible, e.g., the standard potentials of the fourth electron uptake. Experimentally, the formation of the 2−, 3−, and 4− anions is not observed in the vacuum.[11,12] The third reduction process was here observed in DMF, liq-DMA, liq-MA, and liq-NH_3 solvents, and our experiments highlighted the important role of countercation size on the energetics of trianion formation: small cations such as tetramethylammonium or lithium ion are assumed to stabilize the reduced species through the formation of ion pairs with the $\mathbf{C}^{3-}$ species. Calculations were therefore carried out in order to test this hypothesis.

Such calculations have been performed in the frame of a *supermolecule-solvated* approach, where the ion pair cluster (supermolecule), between the anions of **C** and the electrolyte cation (i.e., Li^{+}, TMA^{+}, and TBA^{+} cation; see Figure 5), has been explicitly taken into account in the MO-SCF calculation. The basis set superposition error (BSSE) was also included. As one might expect, the minimum-energy arrangement for [$\mathbf{C}^{-}$/TMA^{+}] has the cation sitting inside the bowl (concave face), whereas the larger cation in [$\mathbf{C}^{-}$/TBA^{+}] prefers the convex face (Figure 5). Thus, the theoretical redox potentials have been obtained by using the calculated relevant quantities of the supermolecule in the thermodynamic cycle of Scheme 1.

If we compare the $E°$(III) values (Table 3), it can be seen that the theoretical value calculated considering the [$\mathbf{C}^{2-}$/TMA^{+}]/[$\mathbf{C}^{3-}$/TMA^{+}] cluster couple falls at the edge of the experimental available potential window. Anyway, the theoretical value was found to be 2.12 V more positive than the value obtained using the solvation energy values of **C** which, in turn, were calculated by employing only the CPCM solvent contribution. Whereas in the case of the [$\mathbf{C}^{2-}$/TBA^{+}]/[$\mathbf{C}^{3-}$/TBA^{+}] cluster (fourth line in Table 3) the theoretical value was found to be 0.31 V more negative than the case of TMA^{+} electrolyte.[46] The same theoretical approach was also used for the DMF with Li^{+} electrolyte, and the standard potentials obtained for the various reductions are in good agreement with the experimental ones.

DFT Calculations at Higher Level of Theory. In order to improve the matching of the theoretical and experimental results, the reduction potentials of corannulene in the various solvents have been calculated, using a higher DFT level of theory approach (B3LYP/cc-pVTZ//B3LYP/6-31G**), which includes also the case of the ion pair cluster formation with Li^{+} in DMF. It should be noted that extremely long calculation time, as well as difficulties in scf convergency, made the corannulene/TBA^{+} and the corannulene/TMA^{+} clusters intractable systems. The results are collected in Table 4. The temperature is accounted for both in the calculation of the solvation free energy and in the calculation of the $\Delta G°_{evr,gas}$ term (see the Computational Details section). The values obtained at B3LYP/cc-pVTZ//B3LYP/6-31G** are remarkably less overestimated (i.e., less negative values) than the corresponding standard potentials calculated by B3PW91/Midi (see Table 3), although they show the same general trend. In particular, the values of the fourth reduction, in the various solvents, continue to be largely out of the useful potential window. However, it is noteworthy to observe that, in the case of Li^{+}/DMF, the data produced by both levels of theory are extremely close to each other and in very good agreement with the experimental ones, most likely due to the higher charge density of the lithium cation compared to the alkylammonium cations, thus suggesting the existence of a leading stabilizing electrostatic contribution.

TABLE 4: Theoretical Reduction Standard Potentials, vs SCE (0.241 V vs NHE), Calculated at the B3LYP/cc-pVTZ//B3LYP/6-31G Level of Theory (Including the BSSE Correction for the Li^{+}/DMF) Using Scheme 1**

solvent	$E°$(I)/V	$E°$(II)/V	$E°$(III)/V	$E°$(IV)/V
ACN (T = 298 K)	−2.17	−3.12	−3.63	−4.52
THF (T = 298 K)	−2.30	−3.69	−4.43	−5.74
DMF (T = 298 K)	−1.99	−2.80	−3.14	−3.98
DMF (T = 213 K)	−2.10	−2.72	−3.09	−3.87
Li^{+}/DMF[a] (T = 213 K)	−1.67	−2.47	−[b]	−[b]
Li^{+}/DMF[c] (T = 213 K)	−1.80	−2.27	−[b]	−[b]
liq-NH_3 (T = 213 K)	−2.12	−2.83	−3.23	−4.15
liq-DMA (T = 193 K)	−2.05	−2.78	−3.06	−3.85

[a] B3LYP/cc-pVTZ//UB3PW91/Midi. [b] The data are not available because the calculations failed to achieve SCF convergence with the BSSE correction. [c] Restricted open-shell B3LYP/cc-pVTZ//UB3PW91/Midi.

All in all, a rather good agreement is obtained between the experimentally observed ion pairing effect and the relevant theoretical predictions.

It must be emphasized that the use of basis sets featuring diffuse functions, 6-31+G* and Aug-cc-pVTZ basis calculations, leads to results which are not physically acceptable, as already reported in the literature.[47] This failure of, in principle, "more accurate" theoretical methods likely stems from the fact that the use of extended basis sets, for instance by using the diffuse function, probably reproduces a *molecule-plus-one-almost-independent-electron* physical view, while a stable anion in solution *experiences* a much stronger interaction between the parent neutral closed-shell species and the added electron. In fact, anions bearing multiple negative charges can be observed electrochemically due to the solvent electrostatic stabilization; on the contrary, they cannot be observed in the vacuum.

Moreover, extended basis sets yield virtual MOs featuring very large AO coefficients, which in turn induce unreliable calculations of electron correlation effects by using methods that are themselves based on the use of virtual orbitals (e.g., Möller−Plesset based methods, which in principle are more accurate, and also much more calculation time-consuming, than the DFT-based ones).

Conclusions

For the first time, the electrochemically reversible reduction of corannulene up to the trianion is reported, and all of the reduction processes have been thoroughly investigated in a variety of "conventional" and "exotic" solvents, using a variety of supporting electrolytes. The collected experimental evidence suggests that production of the trianion is largely influenced by ion pairing stabilization occurring between corannulene and countercations from the supporting electrolyte: higher charge density alkylammonium (namely, tetramethylammonium) or alkali cations are needed in order to obtain formation of the trianion within the available potential window. These results are in close agreement with theoretical calculations, wherein the ion pairing effect has been modeled considering explicitly the possible formation of the $\mathbf{C}^n$/tetrabutylammonium, $\mathbf{C}^n$/tetramethylammonium, and $\mathbf{C}^n/Li^+$ clusters (with $n = 1-, 2-, 3-, 4-$). It is worth noting that calculations predict that the electrochemical generation of tetraanion cannot be accomplished because of its very negative standard potential that locates the fourth reduction outside the currently available experimental potential windows.

Detailed comparison of the experimental and theoretical results, obtained using different levels of the theory, show that the DFT approach is best for dealing with negatively charged species. Moreover, data obtained at the B3LYP/cc-pVTZ//B3LYP/6-31G** level of theory greatly improve the accuracy of the calculated redox potentials, with respect to B3PW91/Midi data, in the case of the corannulene single molecule. The same does not hold when dealing with cluster calculations, most likely because the electrostatic interaction energy dominates.

Acknowledgment. This research was supported by the University of Bologna, University of Modena e Reggio Emilia, and the United States Department of Energy. INSTM and CINECA are also acknowledged for a computing time grant for the use of the IBM SP5 mainframe.

Supporting Information Available: CV curves of corannulene in TBAH/ACN, TBAH/THF and in DMF solution containing TEAB and $LiAsF_6$; tables with theoretical data, concerning (i) the EA at different level of theory, (ii) the Gibbs free energy (step I in Scheme 1) and the solvation energy of corannulene species and ion pair clusters in different media, and (iii) calculated standard reduction potentials of corannulene in DMF at different levels of theory. This material is available free of charge via the Internet at http://pubs.acs.org.

References and Notes

(1) (a) Scott, L. T. *Pure Appl. Chem.* **1996**, *68*, 291. (b) Rabideau, P. W.; Sygula, A. *Acc. Chem. Res.* **1996**, *29*, 235. (c) Mehta, G.; Rao, H. S. P. *Tetrahedron* **1998**, *54*, 13325. (d) Mehta, G.; Panda, G. *Proc. Indian Natl. Sci. Acad., Part A* **1998**, *64*, 587. (e) Scott, L. T.; Bronstein, H. E.; Preda, D. V.; Ansems, R. B. M.; Bratcher, M. S.; Hagen, S. *Pure Appl. Chem.* **1999**, *71*, 209. (f) Scott, L. T. *Angew. Chem., Int. Ed.* **2004**, *43*, 4994. (g) Wu, Y.-T.; Siegel, J. S. *Chem. Rev.* **2006**, *106*, 4843, and references cited therein.

(2) Lovas, F. J.; McMahon, R. J.; Grabow, J.-U.; Schnell, M.; Mack, J.; Scott, L. T.; Kuczkowski, R. L. *J. Am. Chem. Soc.* **2005**, *127*, 4345.

(3) (a) Anson, J. C.; Nordman, C. E. *Acta Crystallogr. B* **1976**, *32*, 1147. (b) Petrukhina, M. A.; Andreini, K. W.; Mack, J.; Scott, L. T. *J. Org. Chem.* **2005**, *70*, 5713.

(4) (a) Scott, L. T.; Hashemi, H. M.; Meyer, D. T.; Warren, H. B. *J. Am. Chem. Soc.* **1991**, *113*, 7082. (b) Rabideau, P. W.; Abdourazak, A. H.; Folsom, H. E.; Marcinow, Z.; Sygula, A.; Sygula, R. *J. Am. Chem. Soc.* **1994**, *116*, 7891.

(5) (a) Seiders, T. J.; Elliot, E. L.; Grube, G. H.; Siegel, J. S. *J. Am. Chem. Soc.* **1999**, *121*, 7804. (b) Scott, L. T.; Hashemi, M. M.; Bratcher, M. S. *J. Am. Chem. Soc.* **1992**, *114*, 1920. (c) Baldridge, K. K.; Siegel, J. S. *Theor. Chem. Acc.* **1997**, *97*, 67. (d) Seiders, T. J.; Baldridge, K. K.; Grube, G. H.; Siegel, J. S. *J. Am. Chem. Soc.* **2001**, *123*, 517.

(6) (a) Aprahamian, I.; Eisenberg, D.; Hoffman, R. E.; Sternfeld, T.; Matsuo, Y.; Jackson, E. A.; Nakamura, E.; Scott, L. T.; Sheradsky, T.; Rabinovitz, M. *J. Am. Chem. Soc.* **2005**, *127*, 9581. (b) Tsefrikas, V. M.; Scott, L. T. *Chem. Rev.* **2006**, *106*, 4868, and references cited therein. (c) Sygula, A.; Fronczek, F. R.; Sygula, R.; Rabideau, P. W.; Olmstead, M. M. *J. Am. Chem. Soc.* **2007**, *129*, 3842.

(7) Parschau, M.; Fasel, R.; Ernst, K.-H.; Gröning, O.; Brandenberger, L.; Schillinger, R.; Greber, T.; Seitsonen, A. P.; Wu, Y.-T.; Siegel, J. S. *Angew. Chem., Int. Ed.* **2007**, *46*, 8258.

(8) Krusic, P. J.; Wasserman, E.; Keizer, P. N.; Morton, J. R.; Preston, K. F. *Science* **1991**, *254*, 1183.

(9) (a) Morita, Y.; Nishida, S.; Kobayashi, T.; Fukui, K.; Sato, K.; Shiomi, D.; Takui, T.; Nakasuji, K. *Org. Lett.* **2004**, *6*, 11397. (b) Nishida, S.; Morita, Y.; Kobayashi, T.; Fukui, K.; Ueda, A.; Sato, K.; Shiomi, D.; Takui, T.; Nakasuji, K. *Polyhedron* **2005**, *24*, 2200.

(10) (a) Petrukhina, M. A.; Andreini, K. W.; Mack, J.; Scott, L. T. *Angew. Chem., Int. Ed.* **2003**, *42*, 3375. (b) Petrukhina, M. A.; Scott, L. T. *Dalton Trans.* **2005**, 2969. (c) Petrukhina, M. A.; Sevryugina, Y.; Rogachev, A. Y.; Jackson, E. A.; Scott, L. T. *Organometallics* **2006**, *25*, 5492. (d) Petrukhina, M. A.; Sevryugina, Y.; Rogachev, A. Y.; Jackson, E. A.; Scott, L. T. *Angew. Chem., Int. Ed.* **2006**, *45*, 7208. (e) Angelici, R. J.; Zhu, B.; Fedi, S.; Laschi, F.; Zanello, P. *Inorg. Chem.* **2007**, *46*, 10901.

(11) Chen, G.; Cooks, R. G.; Corpuz, E.; Scott, L. T. *J. Am. Soc. Mass Spectrom.* **1996**, *7*, 619.

(12) Denifl, S.; Ptasinska, S.; Sonnweber, B.; Scheier, P.; Liu, D.; Hagelberg, F.; Mack, J.; Scott, L. T.; Mark, T. D. *J. Chem. Phys.* **2005**, *123*, 104308.

(13) (a) Janata, J.; Gendell, J.; Ling, C.-Y.; Barth, W.; Backes, L., Jr.; Lawton, R. G. *J. Am. Chem. Soc.* **1967**, *89*, 3056. (b) Seiders, T. J.; Baldridge, K. K.; Siegel, J. S.; Gleiter, R. *Tetrahedron Lett.* **2000**, *41*, 4519.

(14) Baumgarten, M.; Gherghel, L.; Wagner, M.; Weitz, A.; Rabinovitz, M.; Cheng, P.-C.; Scott, L. T. *J. Am. Chem. Soc.* **1995**, *117*, 6254.

(15) (a) Xie, Q.; Perez-Cordero, E.; Echegoyen, L. *J. Am. Chem. Soc.* **1992**, *114*, 3978. (b) Paolucci, F.; Marcaccio, M.; Roffia, S.; Orlandi, G.; Zerbetto, F.; Prato, M.; Maggini, M.; Scorrano, G. *J. Am. Chem. Soc.* **1995**, *117*, 6572. (c) Bendikov, M.; Wudl, F.; Perepichka, D. F. *Chem. Rev.* **2004**, *104*, 4891.

(16) Ayalon, A.; Sygula, A.; Cheng, P.-C.; Rabinovitz, M.; Rabideau, P. W.; Scott, L. T. *Science* **1994**, *265*, 1065.

(17) Ayalon, A.; Rabinovitz, M.; Cheng, P.-C.; Scott, L. T. *Angew. Chem., Int. Ed.* **1992**, *31*, 1636.

(18) Benassi, R. *Theor. Chem. Acc.* **2001**, *106*, 259.

(19) Scott, L. T.; Cheng, P.-C.; Hashemi, M. M.; Bratcher, M. S.; Meyer, D. T.; Warren, H. B. *J. Am. Chem. Soc.* **1997**, *119*, 10963.

(20) (a) Saji, T.; Yamada, T.; Aoyagui, S. *J. Electroanal. Chem.* **1975**, *61*, 147. (b) Marcaccio, M.; Paolucci, F.; Paradisi, C.; Carano, M.; Roffia, S.; Fontanesi, C.; Yellowlees, L. J.; Serroni, S.; Campagna, S.; Balzani, V. *J. Electroanal. Chem.* **2002**, *532*, 99.

(21) (a) La Pensée, A. A.; Bickley, J.; Higgins, S. J.; Marcaccio, M.; Paolucci, F.; Roffia, S.; Charnock, J. M. *J. Chem. Soc., Dalton Trans.* **2002**, 4095. (b) Cecchet, F.; Gioacchini, A. M.; Marcaccio, M.; Paolucci, F.; Roffia, S.; Alebbi, M.; Bignozzi, C. A. *J. Phys. Chem. B* **2002**, *106*, 3926. (c) Guldi, D. M.; Maggini, M.; Menna, E.; Scorrano, G.; Ceroni, P.; Marcaccio, M.; Paolucci, F.; Roffia, S. *Chem.—Eur. J.* **2001**, *7*, 1597.

(22) Bard, A. J.; Faulkner, L. R. *Electrochemical Methods. Fundamentals and Applications*, 2nd ed.; Wiley: New York, 2001.

(23) Yee, E. L.; Cave, R. J.; Guyer, K. L.; Tyma, P. D.; Weaver, M. J. *J. Am. Chem. Soc.* **1979**, *101*, 1131.

(24) Amatore, C.; Lefrou, C. *J. Electroanal. Chem.* **1992**, *324*, 33.

(25) Antigona developed by Dr. Loïc Mottier, University of Bologna, Bologna, Italy, 1999.

(26) Spieser, B. In *Electroanalytical Chemistry. A Series of Advances*; Bard, A. J., Rubistein, I., Eds.; Marcel Dekker: New York, 1996; Vol. 19, p 1, and references therein.

(27) Frisch, M. J.; Trucks, G. W.; Schlegel, H. B.; Scuseria, G. E.; Robb, M. A.; Cheeseman, J. R.; Montgomery, J. A., Jr.; Vreven, T.; Kudin, K. N.; Burant, J. C.; Millam, J. M.; Iyengar, S. S.; Tomasi, J.; Barone, V.; Mennucci, B.; Cossi, M.; Scalmani, G.; Rega, N.; Petersson, G. A.; Nakatsuji, H.; Hada, M.; Ehara, M.; Toyota, K.; Fukuda, R.; Hasegawa, J.; Ishida, M.; Nakajima, T.; Honda, Y.; Kitao, O.; Nakai, H.; Klene, M.; Li, X.; Knox, J. E.; Hratchian, H. P.; Cross, J. B.; Bakken, V.; Adamo, C.;

Jaramillo, J.; Gomperts, R.; Stratmann, R. E.; Yazyev, O.; Austin, A. J.; Cammi, R.; Pomelli, C.; Ochterski, J. W.; Ayala, P. Y.; Morokuma, K.; Voth, G. A.; Salvador, P.; Dannenberg, J. J.; Zakrzewski, V. G.; Dapprich, S.; Daniels, A. D.; Strain, M. C.; Farkas, O.; Malick, D. K.; Rabuck, A. D.; Raghavachari, K.; Foresman, J. B.; Ortiz, J. V.; Cui, Q.; Baboul, A. G.; Clifford, S.; Cioslowski, J.; Stefanov, B. B.; Liu, G.; Liashenko, A.; Piskorz, P.; Komaromi, I.; Martin, R. L.; Fox, D. J.; Keith, T.; Al-Laham, M. A.; Peng, C. Y.; Nanayakkara, A.; Challacombe, M.; Gill, P. M. W.; Johnson, B.; Chen, W.; Wong, M. W.; Gonzalez, C.; Pople, J. A. *Gaussian 03, revision C.02*; Gaussian, Inc.: Wallingford, CT, 2004.

(28) Winget, P.; Weber, E. J.; Cramer, C. J.; Truhlar, D. G. *Phys. Chem. Chem. Phys.* **2000**, *2*, 1231.

(29) Baik, M.; Friesner, R. *J. Phys. Chem. A* **2002**, *106*, 7407.

(30) Barone, V.; Cossi, M. *J. Phys. Chem. A* **1998**, *102*, 1995.

(31) Miertus, S.; Scrocco, E.; Tomasi, J. *Chem. Phys.* **1981**, *55*, 117.

(32) *Handbook of Chemistry and Physics*, 75th ed.; CRC: Boca Raton, FL, 1994.

(33) I.e., ZPE and vibrational contribution at each specific temperature and for each specific electronic state; in the latter case, unscaled frequency values were used.

(34) The reduction potentials for the first and second process, reported by Janata (ref 13a), are E(I) $=-1.93$ V, E(II) $=-2.41$ V (polarography technique) and by Seiders (ref 13b) are E(I) $=-1.91$ V, E(II) $=-2.48$ V (OSW voltammetry). Such values have been recalculated versus SCE for comparison purposes, from the corresponding original ones versus Ag/AgCl, considering that Ag/AgCl is -0.045 V versus SCE (ref 22).

(35) Fawcett, W. R.; Fedurco, M. *J. Phys. Chem.* **1993**, *97*, 7075.

(36) (a) Kalinowski, M. K. *Chem. Phys. Lett.* **1970**, *7*, 55. (b) Lasia, A. *J. Electroanal. Chem.* **1972**, *36*, 511. (c) Kapturkiewicz, A.; Opallo, M. *J. Electroanal. Chem.* **1985**, *185*, 15. (d) Fry, A. J. *Electroanalysis* **2006**, *18*, 391.

(37) Fontanesi, C.; Benassi, R.; Giovanardi, R.; Marcaccio, M.; Paolucci, F.; Roffia, S. *J. Mol. Struct.* **2002**, *612*, 277.

(38) Meerholz, K.; Heinze, J. *J. Am. Chem. Soc.* **1989**, *111*, 2325.

(39) Further investigations concerning the kinetics of the three reductions are currently being undertaken, and the results will be reported in a following paper.

(40) Gruhn, N. E.; Macías-Ruvalcaba, N. A.; Evans, D. H. *J. Phys. Chem. A* **2006**, *110*, 5650.

(41) The presence of the chlorinated precursor of corannulene as impurity (which has been estimated from the CV curve to be 0.03 mM) is not detectable in other solvents because in liq-NH_3 the chlorinated species has a much higher solubility than corannulene, making it to become voltammetrically measurable even though the solid sample contains a very low amount ($\leq$1%) of such precursor impurity.

(42) Sygula, A.; Rabideau, P. W. *J. Mol. Struct. (THEOCHEM)* **1995**, *333*, 215.

(43) During the revision of this paper, a communication was published concerning the flattening and bowl inversion barrier of a corannulene derivative, upon increasing the negative charge, which is in agreement with our results for corannulene, calculated, for the first time, in vacuum and in different solvents. See: Nishida, S.; Morita, Y.; Ueda, A.; Kobayashi, T.; Fukui, K.; Ogasawara, K.; Sato, K.; Takui, T.; Nakasuji, K. *J. Am. Chem. Soc.* **2008**, *130*, 14954.

(44) (a) Trasatti, S. *Pure Appl. Chem.* **1986**, *58*, 955. (b) Tissandier, M. D.; Cowen, K. A.; Feng, W. Y.; Gundlach, E.; Cohen, M. H.; Earhart, A. D.; Coe, J. V. *J. Phys. Chem. A* **1998**, *102*, 7787.

(45) A value of 4.36 eV could be also used for the ΔG°_{ox} term, on the basis of the estimation of the solvation Gibbs energy of H^+ by Tissandier (ref 44b). The result is a constant variation of 0.08 V, i.e., more positive values of E°_{calc}.

(46) UB3PW91/Midi data, when considering the **C**/tetramethylammonium cluster, have been compared with results obtained calculating the EA value in Scheme 1 at the UB3LYP/6-31G* level of theory, which yielded -2.39, -3.03, -3.23, and -5.42 V.

(47) (a) Guerra, M. *Chem. Phys. Lett.* **1990**, *167*, 315. (b) Heinrich, N.; Koch, G.; Frenking, G. *Chem. Phys. Lett.* **1986**, *124*, 20. (c) Fontanesi, C. *J. Mol. Struct. (THEOCHEM)* **1997**, *392*, 87.

JP8045092